Natural Product Sciences
21(4) : 282-288 (2015)
http://dx.doi.org/10.20307/nps.2015.21.4.282

Viriditoxin Induces G2/M Cell Cycle Arrest and Apoptosis in A549 Human Lung Cancer Cells

Ju Hee Park†, Tae Hwan Noh†, Haibo Wang, Nam Deuk Kim, and Jee H. Jung*

College of Pharmacy, Pusan National University, Busan 609-735, Korea

Abstract – Viriditoxin is a fungal metabolite isolated from *Paecilomyces variotii*, which was derived from the giant jellyfish *Nemopilema nomurai.* Viriditoxin was reported to inhibit polymerization of FtsZ, which is a key protein for bacterial cell division and a structural homologue of eukaryotic tubulin. Both tubulin and FtsZ contain a GTP-binding domain, have GTPase activity, assemble into protofilaments, two-dimensional sheets, and protofilament rings, and share substantial structural identities. Accordingly, we hypothesized that viriditoxin may inhibit eukaryotic cell division by inhibiting tubulin polymerization as in the case of bacterial FtsZ inhibition. Docking simulation of viriditoxin to β-tubulin indicated that it binds to the paclitaxel-binding domain and makes hydrogen bonds with Thr276 and Gly370 in the same manner as paclitaxel. Viriditoxin suppressed growth of A549 human lung cancer cells, and inhibited cell division with G2/M cell cycle arrest, leading to apoptotic cell death.
Keywords – Viriditoxin, *Paecilomyces variotii,* FtsZ, Tubulin, G2/M cell cycle arrest, Apoptosis, A549 cells

Introduction

Marine microorganisms are an important source of biologically active and chemically unique secondary metabolites. In our continuing study on bioactive metabolites from jellyfish-derived microorganisms, the extract of the fungal strain *Paecilomyces variotii*, which was isolated from the inner tissue of the jellyfish *Nemopilema nomurai*, showed lethality to brine shrimp larvae (LD_{50} 2 μg/mL) and antibacterial activity against several pathogens. Guided by antibacterial activity, viriditoxin (Fig. 1) was isolated as an antibacterial constituent of the culture of *P. variotii.*[1] It was an interesting molecule due to its broad-spectrum antibiotic activity against Gram-positive pathogens, including methicillin-resistant *Staphylococcus aureus* (MRSA) and vancomycin-resistant *Enterococci* (VRE).[1,2] Viriditoxin was lethal to mice with LD50 of 2.8 mg/kg, and it can activate ATP hydrolysis (ATPase).[3]

Regarding the antibacterial mechanism of action, viriditoxin was defined as an inhibitor of bacterial cell division by blocking filamenting temperature-sensitive mutant Z (FtsZ), which represents an excellent novel target for antibacterial drug discovery. FtsZ is a key protein for bacterial cell division. FtsZ is a structural homologue of eukaryotic tubulin, which forms microtubules during cell division and plays a central role in the cytokinesis of cells.[4,5] Both tubulin and FtsZ contain a GTP-binding domain, have GTPase activity, assemble into protofilaments, two-dimensional sheets, and protofilament rings, and share substantial structural identities.[6] FtsZ polymerizes in a nucleotide-dependent manner head-to-tail to form single-stranded filaments that assemble into a contractile ring.[7] The ring is called the z-ring and forms on the inside of the cytoplasmic membrane where it marks the future site of the septum of a dividing bacterial cell. Although FtsZ polymerization rapidly reaches steady state, the z-ring is dynamically maintained through the course of cell division by continuous and rapid turnover of FtsZ polymers, likely fueled by FtsZ's GTP hydrolysis. The nature of FtsZ polymers in vivo is unknown but FtsZ can form tubules, sheets, and mini rings in vivo. The three dimensional structure of FtsZ is similar to the structure of α- and β-tubulin. Nucleotide binding is very similar between FtsZ and β-tubulin, with many residues involved in GDP binding being conserved.[4]

Viriditoxin was reported to inhibit FtsZ polymerization of *E. coli*, affecting cell morphology, macromolecular synthesis, and DNA-damage response.[2,8,9] Accordingly, we hypothesized that viriditoxin may inhibit eukaryotic cell division by blocking tubulin polymerization as it inhibit bacterial cell division by blocking FtsZ polymeri-

*Author for correspondence
Jee H. Jung, College of Pharmacy, Pusan National University, Busan 609-735, Korea
Tel: +82-51-510-2803; E-mail: jhjung@pusan.ac.kr

†These authors equally contributed.

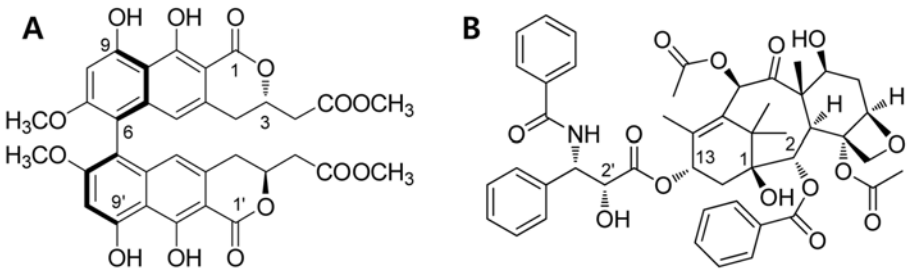

Fig. 1. Chemical structures of viriditoxin (**A**) and paclitaxel (**B**).

zation. Although viriditoxin was initially identified by its activity against the purified *E. coli* (Gram-negative) FtsZ protein, activity of viriditoxin against many Gram-positive bacteria indicates high functional conservation of the target in these clinically important pathogens. Presumably, the structure of the FtsZ molecule is very highly conserved in the pocket that is engaged by viriditoxin, and this may limit the ability to develop cross resistance in the pathogenic bacteria.

There was also a contradictory report that FtsZ inhibitors including viriditoxin and the drug development candidate PC190723 did not inhibit GTPase activity.[10] GTP analogs with small hydrophobic substituents at C-8 of the nucleobase efficiently inhibit FtsZ polymerization, whereas they have an opposite effect on the polymerization of tubulin. So it was suggested that the GTP binding sites formed by association of FtsZ monomers and α,β-tubulin heterodimers are different.[11] Later it was also proposed that small molecule FtsZ inhibitors including viriditoxin inhibit cell division by inducing changes in the physicochemical properties of membrane rather than by specific effect on FtsZ. The physicochemical activity of these molecules leads to delocalization of membrane-associated proteins, which perturbs pathways involved in division and cell shape and may be ultimately responsible for the phenotypes observed in vivo.[12]

Curcumin was described as inhibitors for both FtsZ and tubulin.[13,14] However, several tubulin inhibitors (albendazole, colchicine, nocodazole, paclitaxel, 3-methoxybenzamide, and thiabendazole) did not show FtsZ inhibition nor GTPase inhibition.[15] There is also a report that cephalochromin (bis naphtho-γ-pyrone) which has similar skeleton with viriditoxin (bis naphtho-α-pyrone), induce G0/G1 cell cycle arrest and apoptosis in A549 human non-small-cell lung cancer by inflicting mitochondrial disruption.[16]

Lung cancer has been the most common cancer for several decades and the most common cancer among men worldwide. Non-small-cell lung cancer constitutes around 80% of lung malignancies, and the 5-year survival of this highly aggressive disease is only 15%.[17] Therefore, there is a substantial need to discover and develop more effective and less toxic antitumor treatments for lung cancer. Viriditoxin showed antitumor activity and effectively inhibited proliferation of prostate cancer cells through cell cycle arrest at the G2/M phase and autophagic cell death.[18] However, its antitumor activity was not fully investigated. Therefore, viriditoxin as an FtsZ inhibitor can be considered as an attractive candidate for tubulin inhibitor. In the present study, we analyzed docking of viriditoxin to β-tubulin, and investigated whether viriditoxin can block cell cycle and suppress proliferation of A549 human non-small-cell lung cancer cells.

Experimental

Isolation of viriditoxin – Viriditoxin was isolated in our Lab, College of Pharmacy, Pusan National University, South Korea. The culture medium and mycelia of the fungus *Paecilomyces variotii* were extracted with EtOAc at room temperature. The EtOAc extract was further partitioned between aqueous MeOH and *n*-hexane. Viriditoxin which cannot be dissolved in both solvents was obtained a yellow precipitate. The chemical structure of viriditoxin was confirmed by NMR analysis. Viriditoxin was dissolved in dimethyl sulfoxide (DMSO) as a stock solution at a 10 mM concentration and was stored at −20 °C.

Reagents – Paclitaxel, docetaxel, and colchicine were purchased from Sigma-Aldrich Co. (St. Louis, MO, USA). Dulbecco's phosphate-buffered saline (DPBS), fetal bovine serum (FBS), trypsin-EDTA were purchased from Gibco Invitrogen Corporation (Carlsbad, CA, USA). WST (EZ-CyTox, Daeil Lab Service Co., Ltd, Seoul, South Korea). The Annexin V-FITC apoptosis detection kit I (cat. no. 556547) was purchased from BD Biosciences (San Diego, CA, USA).

Docking analysis – AutoDock Vina 1.1.2 software

(The Scripps Research Institute, La Jolla, CA, USA) was used for docking simulation. Protein coordinate was downloaded from Protein Data Bank (protein code number: 1JFF). Electrostatic charges of the assigned atoms were calculated as Gasteiger charges. After preparing a receptor, Chemdraw 12.0 (Cambridge Soft Corporation, Cambridge, MA, USA) was used to draw ligands. All ligands were added electrostatic charge by using MGLTools 1.5.4 (The Scripps Research Institute, La Jolla, CA, USA). Size of grid box (searching space) was calculated in Chimera 1.10.1 software. After docking simulation, PyMol v1.7 (Schrodinger LLC, New York, NY, USA) was used as visualizer, and investigation of ligand-receptor interactions. Also Ligand Scout 3.12 (Inte:Ligand, Austria, Europe) was used to study pharmacophore. Before exploring amino acid which makes hydrogen bond with ligand, MMFF94 minimization was performed.

Cell culture – The human lung cancer A549 cells were provided by professor Jin Wook Yoo, Lab. of Drug Delivery, College of Pharmacy, Pusan National University, South Korea and cultured in RPMI-1640 (Wel Gene) supplemented with 10% heat-inactivated fetal bovine serum (FBS, Gibco), 2 mM glutamine (Sigma-Aldrich), 100 U/ml penicillin (HyClone) and 100 μg/ml streptomycin (HyClone) at 37 ºC in a humidified 5% CO_2.

Cell viability assay – Cell viability was determined using WST (EZ-CyTox, Daeil Lab Service Co., Ltd, Seoul, South Korea). The Cells (1×10^4) were seeded in 96 well plates of flat bottom in a final volume of 100 μL/well culture medium and incubated at 37 ºC for 24 h. Then, cells were treated with different concentration of viriditoxin, paclitaxel, or colchicine for 24 h. After treatment, WST reagent (10 μL) was added to each well and cells were cultured for additional 1 h. Then, the plate was shaked thoroughly for 1 min. The absorbance of samples was measured under a wavelength of 450 nm using an ELISA plate reader.

Analysis of cell cycle by flow cytometry – Cells were treated with viriditoxin (2.5, 5, 10 and 20 μM) or paclitaxel, colchicine (20 μM) for 24 h. Cells (1×10^6) were harvested by centrifugation, washed once with PBS, and fixed in 75% ethanol at –20 ºC overnight. Fixed cells were prepared for flow cytometry analysis by washing twice with PBS and then treated with RNase A (100 μg/ml in PBS, 30 min, 37 ºC). After incubation, the cells were stained with 10 μg/ml propidium iodide (PI, Sigma-Aldrich). DNA content was analyzed by flow cytometry (BD Accuri™ C6, Becton-Dickinson, San Jose, CA, USA), and results were displayed as histograms of DNA content.

Annexin V-FITC binding assay – The Annexin V-FITC binding assay was performed according to the manufacturer's instruction using the Annexin V-FITC detection kit I (BD Biosciences, San Diego, CA, USA). The cells were treated with viriditoxin, paclitaxel, or colchicine for 24 h. Cells (1×10^6) harvested were washed twice with cold PBS, suspended the cells in 1x binding buffer and incubated with 5 μL of FITC-conjugated Annexin-V and 5 μL of propidium iodide (PI) for 15 min at room temperature in the dark. Binding buffer (1x, 400 μL) was added to each sample tube, and immediately the samples were analyzed by FACS (Becton-Dickinson).

Results and Discussion

Docking of viriditoxin to tubulin – To investigate potential binding mode of viriditoxin, docking simulation was performed using AutoDock Vina. Docking of viriditoxin was performed employing large searching space, and several potential binding domains were examined. When the docking results were arranged in order of frequency, viriditoxin binding domain (Fig. 2B) was mostly overlapped with paclitaxel binding domain (Fig. 2A). Paclitaxel binding domain of bovine β-tubulin was well defined by crystallography but the binding conformation is still not fully understood.[19] The T-taxol conformation, which was proposed as the bioactive conformation of paclitaxel (PTX), was employed to investigate hydrogen bonding, and paclitaxel was shown to form hydrogen bonds with Thr276 and Gly370 of β-tubulin.[20] The oxetane oxygen of paclitaxel makes hydrogen bond with the hydroxyl group of Thr276, and the C-2′ hydroxyl group of paclitaxel makes hydrogen bond with the backbone NH of Gly370 (Fig. 2C). According to docking results, viriditoxin also makes hydrogen bonds with Gly370 and Thr276. The C-9′ hydroxyl group of viriditoxin makes hydrogen bond with Thr276, and the C-1 carbonyl group of α-pyrone of viriditoxin makes hydrogen bond with the backbone NH of Gly370. The affinity score of viriditoxin (–8.4 kcal/mol) was little lower than paclitaxel (–9.2 kcal/mol). Thus, viriditoxin may bind to the paclitaxel binding domain of β-tubulin and exhibit antimitotic activity by blocking tubulin dynamics, possibly in a similar manner as paclitaxel.

Viriditoxin induced growth inhibition in human cancer cell line A 549 – Human lung cancer cell line A 549 was used as research target because Lung cancer is the most common cause of cancer death in the world. To investigate the effects of viriditoxin on the viability of A549 cells, the growth inhibitory potential was evaluated by the WST (water soluble tetrazolium salts) assay.

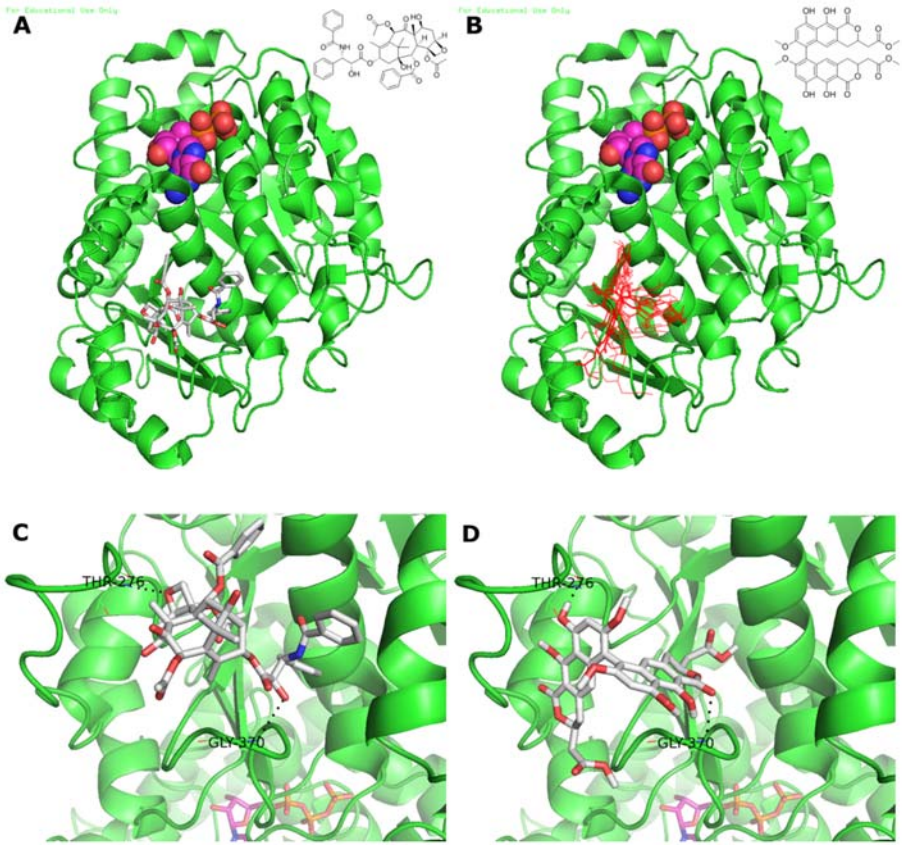

Fig. 2. Binding modes of viriditoxin and paclitaxel to the ligand binding domain of β-tubulin. GDP is presented as ball and stick. (**A**) Co-crystal structure of paclitaxel bound to β-tubulin (PDB code number 1JFF). (**B**) Docking results of viriditoxin to β-tubulin. Viriditoxin binds to the paclitaxel binding domain. (**C**) Paclitaxel interaction with loop of β-tubulin. Oxetane of paclitaxel makes a hydrogen bond with Thr276. The C-2′ hydroxyl group of paclitaxel makes hydrogen bond with the backbone NH of Gly370. (**D**) Model of viriditoxin which makes hydrogen bonds with Gly370 and Thr276. The C-9′ hydroxyl group of viriditoxin makes hydrogen bond with Thr276. The C-1 carbonyl group of α-pyrone of viriditoxin makes hydrogen bond with the backbone NH of Gly370.

Paclitaxel and colchicine were used as a positive control. After 24 h incubation, cells (1×10^4 viable cells/mL) were treated with viriditoxin, paclitaxel, or colchicine at the concentration of 2.5, 5, 10 and 20 μM for 24 h. The absorption values at 450 nm were determined with an ELISA plate reader. Values were normalized to untreated (control) samples. All assays were performed in triplicate. As shown in Fig. 3, after 24 h incubation, viriditoxin inhibit the growth of human lung cancer cells A549 in a concentration-dependent manner with the IC_{50} value of 5.1 μM. At the same experimental condition, the IC_{50} value of paclitaxel and colchicine against A549 cells were 2.3 and 1.9 μM, respectively (Table 1). The cytotoxicity of viriditoxin against A549 cells was quite comparable to that of paclitaxel and colchicine. Viriditoxin also exhibited cytotoxicity against HCT116 (human colon cancer), KB (human nasopharyngeal cancer), and SH-SY5Y (neuroblastoma) with IC_{50} values of 18.0, 2.3, and 12.0 μM, respectively.

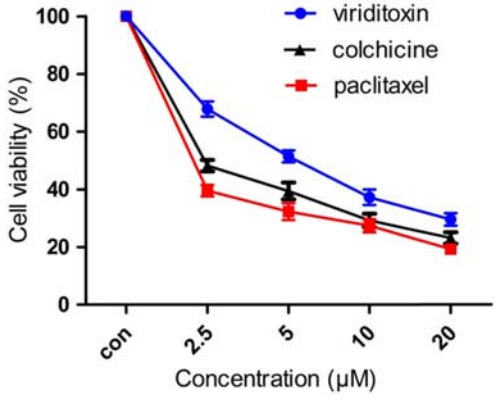

Fig. 3. Effect of viriditoxin, paclitaxel, and colchicine on viability of A549 cells. The cells were treated with viriditoxin, paclitaxel, or colchicine at various concentrations (0-20 μM) for 24 h. The percentage of cell survival was determined as the ratio between treated cells and untreated controls. Results are expressed as mean ± S.E.M., n=3.

Viriditoxin caused G2/M cell cycle arrest in A549 cells – Cell proliferation is generally controlled by the

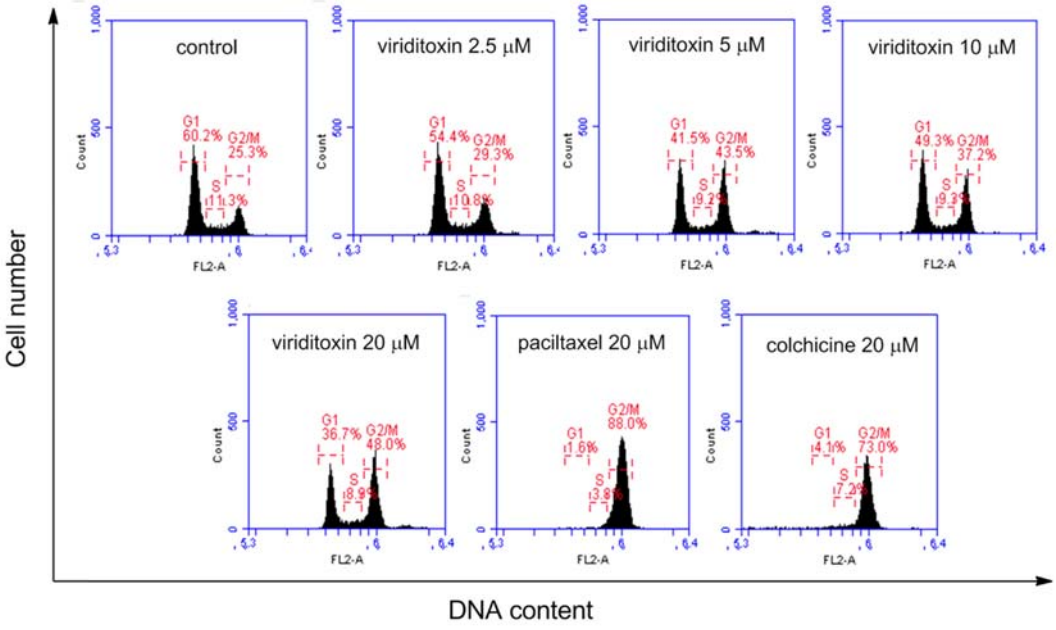

Fig. 4. Cell cycle analysis of A549 cells treated with viriditoxin, paclitaxel, or colchicine. A549 cells were treated for 24 h with viriditoxin (0-20 μM), paclitaxel (20 μM) or colchicine (20 μM). The cells were fixed and digested with RNase, and then cellular DNA was stained with PI and analyzed by flow cytometry. The percentages of cells in G0/G1, S, and G2/M phases of cell cycle were shown.

progression of three distinctive phases (G0/G1, S, and G2/M) of the cell cycle and cell-cycle arrest is considered one of the most common causes of the inhibition of cell proliferation. To examine whether viriditoxin induced growth inhibition was associated with cell cycle regulation, the cell cycle distribution was analyzed by flow cytometry. Effects of paclitaxel and colchicine on cell cycle distribution were also evaluated in the same condition. A 549 cells were incubated with various concentrations of viriditoxin (2.5, 5, 10, 20 μM), paclitaxel (20 μM), or colchicine (20 μM) for 24 h. As shown in Fig. 4, viriditoxin significantly increased G2/M phase of cells in a concentration-dependent manner and concomitantly decreased the cells in the S phase (Fig. 4). An accumulation of cells in G2/M phase of 29.3%, 37.2%, 43.5%, and 48% was observed at the concentration of 2.5, 5, 10, and 20 μM, respectively, when compared with 25.3% of untreated (control) cells (Table

Table 1. The IC_{50} (μM) values of viriditoxin and mitotoxins on A549 human lung cancer cells

Viriditoxin	Colchicine	Paclitaxel
5.1 ± 0.4	2.3 ± 0.5	1.9 ± 0.3

A549 cells were treated with viriditoxin, paclitaxel, or colchicine at various concentrations (2.5, 5, 10, and 20 μM) for 24 h. The IC_{50} values were expressed as the mean ± SEM of three independent determinations.

Table 2. Effect of viriditoxin and mitotoxins on cell cycle distribution in A549 cells

		Cell cycle (% total cells)		
		G1	S	G2/M
Control (μM)		60.2 ± 0.3	11.3 ± 0.5	25.3 ± 0.2
viriditoxin	2.5	54.4 ± 0.4	10.8 ± 0.3	29.3 ± 0.3
	5	49.3 ± 0.2	9.3 ± 0.7	37.2 ± 0.5
	10	41.5 ± 0.3	9.2 ± 0.4	43.5 ± 1.0
	20	36.7 ± 0.3	8.9 ± 0.2	48.0 ± 0.9
Paclitaxel (20 μM)		1.6 ± 0.2	3.8 ± 0.3	88 ± 0.4
Colchicine (20 μM)		3.7 ± 0.3	9.3 ± 0.6	73.5 ± 0.3

A549 cells were treated for 24 h with viriditoxin (0-20 μM), paclitaxel (20 μM), or colchicine (20 μM). Cells were then fixed and stained with propidium iodide to analyze DNA content using flow cytometry. Data are expressed as mean ± SEM of three independent determinations.

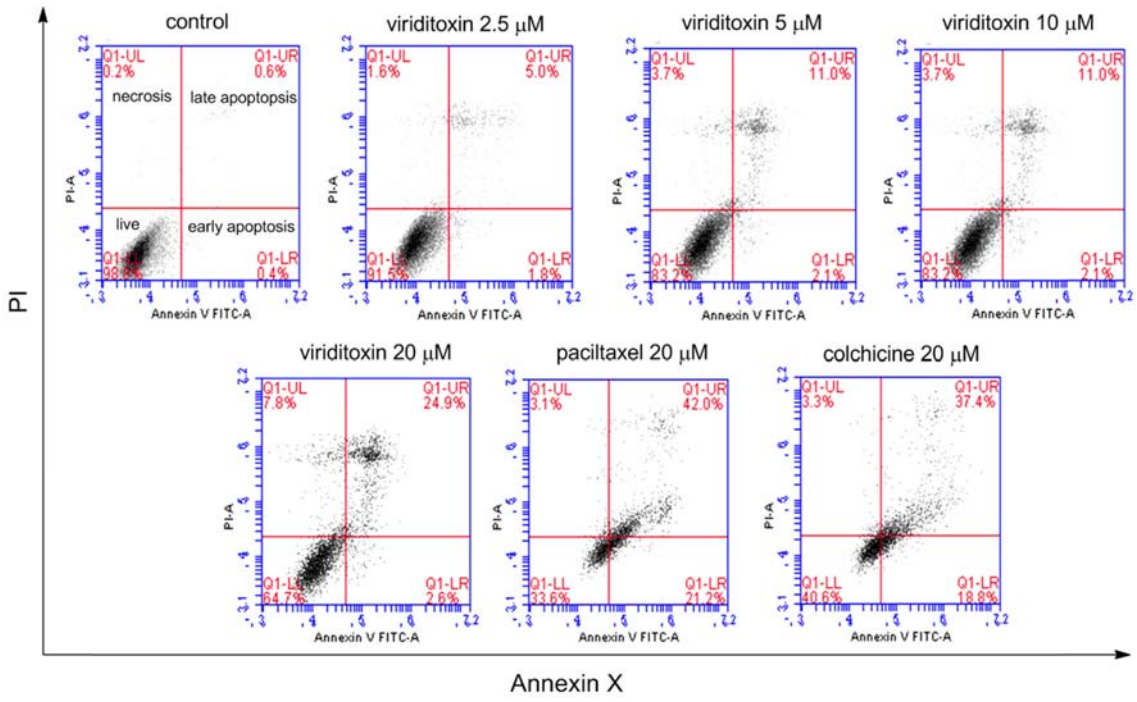

Fig. 5. Effect of viriditoxin, paclitaxel, and colchicine on apoptosis of A549 cells. Viriditoxin-induced apoptosis in A549 cells was examined by Annexin V-PI binding assay. A549 cells were treated with viriditoxin, paclitaxel, or colchicine for 24 h at different concentrations as indicated. Representative flow cytometry scatter plots depict percent Annexin V/PI staining at 24 h after viriditoxin treatment. Apoptotic cell death was analyzed using flow cytometry.

Table 3. Effect of viriditoxin and mitotoxins on apoptosis in A549 cells

		Live	Early apoptosis	Late apoptosis	Necrosis
Control (μM)		98 ± 0.1	0.4 ± 0.2	0.6 ± 0.1	0.2 ± 0.1
viriditoxin	2.5	91.5 ± 0.2	1.8 ± 0.3	5 ± 0.2	1.6 ± 0.3
	5	83.2 ± 0.2	2.1 ± 0.2	11 ± 0.4	3.7 ± 0.6
	10	77.6 ± 0.5	2.1 ± 0.4	14.7 ± 0.1	5.5 ± 0.4
	20	64.7 ± 0.4	2.6 ± 0.2	24.9 ± 0.3	7.8 ± 0.8
Paclitaxel (20 μM)		33.6 ± 1.1	21.2 ± 0.6	42 ± 0.4	3.1 ± 0.2
Colchicine (20 μM)		40.6 ± 0.7	18.8 ± 0.7	37.4 ± 0.5	3.3 ± 0.3

A549 cells were treated for 24 h with viriditoxin (0-20 μM), paclitaxel (20 μM), or colchicine (20 μM). Cells were stained with Annexin V/PI. Data are expressed as mean ± SEM of three independent determinations.

2). Thus, viriditoxin inhibited the growth of A 549 cells by arresting cells in the G2/M phases.

Viriditoxin induced apoptosis in A549 cells – The apoptosis-induction of viriditoxin was examined using Annexin V-FITC/PI staining and flow cytometric analysis. Annexin V-FITC/PI staining can differentiate cells of early or late stage of apoptosis as well as necrotic cells. Viable cells with intact membranes exclude PI, whereas the membranes of dead and damaged cells are permeable to PI. For example, viable cells are FITC Annexin V and PI negative, cells that are in early apoptosis are FITC Annexin V positive and PI negative. Cells that are in late apoptosis or already dead cells are both FITC Annexin V and PI positive. A549 cells were treated with viriditoxin, paclitaxel, or colchicine for 24 h. Exposure of A549 cells to viriditoxin (2.5, 5, 10, 20 μM), paclitaxel, or colchicine (20 μM) generally resulted in an increase in the percentages of late apoptotic (Annexin V+/PI+) and necrotic cells, and a reduction in the percentage of intact cells when compared with the control (Fig. 5). The percentage of apoptotic cells was increased compared to control at 24 h (Table 3). It would be necessary to further confirm

apoptosis by using immunostaining or live fluorescence imaging that the same cells are indeed showing 'PS-eat-me signals' and 'JC-1 monomer signals' as well as characteristic morphology of apoptotic DNA.

In conclusion, present results show that viriditoxin significantly inhibited proliferation of A549 lung cancer cells via inducing G2/M phase cell cycle arrest and apoptosis. Further study on direct effect of viriditoxin on tubulin is in progress.

Acknowledgments

This research was a part of the project entitled 'Omics based fishery disease control technology development and industrialization' funded by the Ministry of Oceans and Fisheries, Korea.

References

(1) Liu, J.; Li, F.; Kim, E. L.; Hong, J. K.; Jung, J. H. *Nat. Prod. Sci.* **2013**, *19*, 61-65.
(2) Wang, J.; Galgoci, A.; Kodali, S.; Herath, K. B.; Jayasuriya, H.; Dorso, K.; Vicente, F.; González, A.; Cully, D.; Bramhill, D.; Singh, S. *J. Biol. Chem.* **2003**, *278*, 44424-44428.
(3) Wong, D. T.; Hamill, R. L. *Biochem. Biophys. Res. Commun.* **1976**, *71*, 332-338.
(4) Löwe, J.; Amos, L. A. *Nature* **1998**, *391*, 203-206.
(5) Tian, W.; Xu, D.; Deng, Y. C. *Pharmazie* **2012**, *67*, 811-816.
(6) Erickson, H. P. *Cell* **1995**, *80*, 367-370.
(7) Bi, E. F.; Lutkenhaus, J. *Nature* **1991**, *354*, 161-164.
(8) Chen, Y.; Erickson, H. P. *J. Biol. Chem*. **2005**, *280*, 22549-22554.
(9) Popp, D.; Iwasa, M.; Erickson, H. P.; Narita, A.; Maéda, Y.; Robinson, R. C. *J. Biol. Chem*. **2010**, *285*, 11281-11289.
(10) Anderson, D. E.; Kim, M. B.; Moore J. T.; O'Brien, T. E.; Sorto, N. A.; Grove, C. I.; Lackner, L. L.; Ames, J. B.; Shaw, J. T. *ACS Chem. Biol.* **2012**, *7*, 1918-1928.
(11) Läppchen, T.; Pinas, V. A.; Hartog, A. F.; Koomen, G. J.; Schaffner-Barbero, C.; Andreu, J. M.; Trambaiolo, D.; Löwe, J.; Juhem, A.; Popov, A. V; den Blaauwen, T. *Chem. Biol.* **2008**, *15*, 189-199.
(12) Foss, M. H.; Eun, Y. J.; Grove, C. I.; Pauw, D. A.; Sorto, N. A.; Rensvold, J. W.; Pagliarini, D. J.; Shaw, J. T.; Weibel, D. B. *Med. Chem. Commun*. **2013**, *4*, 112-119.
(13) Gupta, K. K.; Bharne, S. S.; Rathinasamy, K.; Naik, N. R.; Panda, D. *FEBS J*. **2006**, *273*, 5320-5332.
(14) Rai, D.; Singh, J. K.; Roy, N.; Panda, D. *Biochem. J*. **2008**, *410*, 147-155.
(15) Wang, J.; Galgoci, A.; Kodali, S.; Herath, K. B.; Jayasuriya, H.; Dorso, K.; Vicente, F.; González, A.; Cully, D.; Bramhill, D.; Singh, S. *J. Biol. Chem.* **2003**, *278*, 44424-44428.
(16) Hsiao, C. J.; Hsiao, G.; Chen, W. L.; Wang, S. W.; Chiang, C. P.; Liu, L. Y.; Guh, J. H.; Lee, T. H.; Chung, C. L. *J. Nat. Prod.* **2014**, *77*, 758-765.
(17) Zhu, Z.; Sun, H.; Ma, G.; Wang, Z.; Li, E.; Liu, Y.; Liu, Y. *Int. J. Mol. Sci.* **2012**, *13*, 2025-2035.
(18) Kundu, S.; Kim, T. H.; Yoon, J. H.; Shin, H. S.; Lee, J.; Jung, J. H.; Kim, H. S. *Int. J. Oncol*. **2014**, *45,* 2331-2340.
(19) Löwe, J.; Li, H.; Downing, K. H.; Nogales, E. *J. Mol. Biol*. **2001**, *313*, 1045-1057.
(20) Sun, L.; Simmerling, C.; Ojima, I. *ChemMedChem* **2009**, *4,* 719-731.

Received August 5, 2015
Revised September 23, 2015
Accepted September 24, 2015